PERGAMON

International Journal of Solids and Structures 36 (1999) 5301–5326

INTERNATIONAL JOURNAL OF SOLIDS and STRUCTURES

www.elsevier.com/locate/ijsolstr

Three-dimensional elasticity solutions to some orthotropic plate problems

T.M. Teo[a,*,1], K.M. Liew[b,2]

[a] *School of Mechanical and Production Engineering, Nanyang Technological University, Nanyang Avenue, Singapore 639798*

[b] *Department of Mechanical Engineering, Massachusetts Institute of Technology, Cambridge, MA 02139, U.S.A.*

Received 23 January 1998; in revised form 21 July 1998; accepted 2 August 1998

Abstract

This paper presents a three-dimensional analysis of rectangular orthotropic plates by employing the differential quadrature (DQ) method. The derivation of the governing equations from the governing equations and the stress–strain relationship of the three-dimensional elasticity model is detailed. The constrained conditions of the orthotropic plate edges are given. The governing equations and boundary conditions are first normalized and discretized according to the DQ procedure. Example problems pertaining to the bending, buckling and free vibration of orthotropic plates with generic boundary conditions are selected to illustrate the simplicity and applicability of the DQ method. The convergence characteristics of the DQ method are first obtained based on numerical studies, after which, the DQ solutions are compared, where possible, with exact solutions. It is found that the DQ method yields accurate results for the plate problems under investigation.

1. Introduction

Conventional numerical methods like the h-version finite element method, the finite difference method, and the boundary element method usually require a large number of grid points for accurate computation of results. Recently, an alternative numerical method, the differential quadrature (DQ) method, was introduced to address this problem. It was found to be rather successful in solving problems in structural mechanics (Bert and Malik, 1996). It was reported that the DQ method was able to rapidly compute accurate solutions for partial differential equations by using only a few grid points in the respective solution domains (Bert et al., 1988a).

* Corresponding author. Fax: 00 65 278 5319; e-mail: tat-ming-teo@hp.com

[1] Present address: Lightwave, SCO, Hewlett-Packard Singapore (Pte) Ltd, 1150 Depot Road, Singapore 109673.

[2] On sabbatical leave from School of Mechanical and Production Engineering, Nanyang Technological University, Nanyang Avenue, Singapore 639798.

0020-7683/99/$ - see front matter
PII: S0020-7683(98)00240-6

The original DQ method was first used for structural mechanics problems by Bert and his associates (Jang, 1987; Bert et al., 1988a, b, 1989; Striz et al., 1988; Jang et al., 1989). Later Quan and Chang (1989a, b) and Shu and Richards (1992) improved on the DQ method by introducing a recurrence relationship which can be used to generate weighting coefficients for any higher-order derivatives. Their method of calculating the weighting coefficients rids the DQ method of ill conditioning problems which have plagued the previous method of obtaining the weighting coefficients. Du et al. (1994) employed this method of calculating the weighting coefficients to study structural mechanics problems.

Prior to the year 1995, the application of the DQ method in structural analysis was limited to Kirchhoff–Love thin plates and Bernoulli–Euler slender beams (Jang, 1987; Chen, 1994; Farsa, 1991; Malik, 1994). Some applications of the DQ method in thick plates were subsequently reported (Han and Liew, 1995; Malik and Bert, 1995). Wang (1995) and Wang et al. (1995) also solved laminated plates and circular plates with varying thickness using the DQ method. In 1997, the application of the DQ method was extended to the three-dimensional free vibration analysis of isotropic plate problems (Teo and Liew, 1997). Teo (1998) used the DQ method to solve bending, buckling and free vibration of three-dimensional isotropic and orthotropic plates. The DQ method was also used by Malik and Bert (1998) to the solution three-dimensional vibration of thick plates.

Numerous methods have been employed by earlier researchers for solving plate problems based on three-dimensional elasticity theory (Srinivas and Rao, 1969, 1970, 1973; Srinivas et al., 1969, 1970; Iyengar et al., 1974; Leissa and Zhang, 1983; Liew et al., 1993, 1994, 1995a, b; Young and Dickinson, 1995). These three-dimensional solutions are extremely useful in evaluating the accuracy of approximate results, for example, in the case of two-dimensional plate theories. To the authors' knowledge, the methods employed by these researchers are either limited to certain boundary conditions or to the plate problem itself. It is the purpose of this paper to provide useful literature on orthotropic plate problems in terms of bending, buckling, and free vibration analyses with generic boundary conditions. The version of the DQ method employed in this study was originated by Quan and Chang (1989a, b), and Shu and Richards (1992). It uses a recurrence formulation to compute the weighting coefficients of higher-order differential equations.

This paper is organised into several sections. First, the DQ approximations are highlighted after which the three-dimensional elasticity equilibrium equations for plate analysis and the boundary conditions are outlined. Next, the normalisation and discretization of the three-dimensional linear elasticity equations and boundary conditions are presented. In the section on numerical results and discussion, the convergence characteristics and accuracy of the DQ method are demonstrated through the solving of numerical test examples for which available exact solutions or numerical values are used for comparison. Finally, some conclusions are drawn from this study.

2. Differential quadrature method

To illustrate the DQ approximation, a one-dimensional function, $f(x)$, shall be used here. According to the DQ method, the nth derivative of a function $f(x)$ can be approximated by

$$\frac{\partial^n f(x)}{\partial x''} = \sum_{j=1}^{N} A_{ij}^{(n)} f(x) \quad \text{for } i = 1, 2, \ldots, N, \quad n = 1, 2, \ldots, N-1 \tag{1}$$

where N is the number of discrete points chosen in the solution domain. The term 'A' represents the weighting coefficient at the ith point in the solution domain. The details for calculating the weighting coefficients as used in this paper can be found in Shu and Richards (1992).

For a multi-dimensional case, each dimension is treated separately. The three-dimensional approximation of a function $f(x, y, z)$ required for the present analysis is shown below (Teo and Liew, 1997):

$$\left.\frac{\partial f}{\partial x}\right|_{ijk} \approx \sum_{l=1}^{N_x} A_{il}^{(1)} f_{ljk}; \quad \left.\frac{\partial f}{\partial y}\right|_{ijk} \approx \sum_{m=1}^{N_y} B_{jm}^{(1)} f_{imk} \tag{2a,b}$$

$$\left.\frac{\partial f}{\partial z}\right|_{ijk} \approx \sum_{n=1}^{N_z} C_{kn}^{(1)} f_{ijn}; \quad \left.\frac{\partial^2 f}{\partial x^2}\right|_{ijk} \approx \sum_{l=1}^{N_x} A_{il}^{(2)} f_{ljk} \tag{2c,d}$$

$$\left.\frac{\partial^2}{\partial y^2}\right|_{ijk} \approx \sum_{m=1}^{N_y} B_{jm}^{(2)} f_{imk}; \quad \left.\frac{\partial^2 f}{\partial z^2}\right|_{ijk} \approx \sum_{n=1}^{N_z} C_{kn}^{(2)} f_{ijn} \tag{2e,f}$$

$$\left.\frac{\partial}{\partial x}\left(\frac{\partial f}{\partial y}\right)\right|_{ijk} \approx \sum_{l=1}^{N_x} A_{il}^{(1)} \sum_{m=1}^{N_y} B_{jm}^{(1)} f_{lmk} \tag{2g}$$

$$\left.\frac{\partial}{\partial x}\left(\frac{\partial f}{\partial z}\right)\right|_{ijk} \approx \sum_{l=1}^{N_x} A_{il}^{(1)} \sum_{n=1}^{N_z} C_{kn}^{(1)} f_{ljn} \tag{2h}$$

$$\left.\frac{\partial}{\partial y}\left(\frac{\partial f}{\partial z}\right)\right|_{ijk} \approx \sum_{m=1}^{N_y} B_{jm}^{(1)} \sum_{n=1}^{N_z} C_{kn}^{(1)} f_{imn} \tag{2i}$$

In the above equations [eqns (2)], A, B and C denote the weighing coefficients at the ith, jth and kth point for the partial derivative of the function with respect to the x, y and z solution domain, respectively. N_x, N_y, and N_z are the total number of discrete points chosen in the x-, y- and z-directions.

3. Basic equations

3.1. Governing equations

The equations of motion for an object in the x-, y-, and z-directions without body force (Srinivas and Rao, 1970; Wittrick, 1987) can be written as:

$$\frac{\partial \sigma_x}{\partial x} + \frac{\partial \tau_{xy}}{\partial y} + \frac{\partial \tau_{xz}}{\partial z} = P_x \frac{\partial^2 u}{\partial x^2} + P_y \frac{\partial^2 u}{\partial y^2} + \rho\omega^2 u \tag{3}$$

$$\frac{\partial \tau_{xy}}{\partial x} + \frac{\partial \sigma_y}{\partial y} + \frac{\partial \tau_{yz}}{\partial z} = P_x \frac{\partial^2 v}{\partial x^2} + P_y \frac{\partial^2 v}{\partial y^2} + \rho\omega^2 v \tag{4}$$

$$\frac{\partial \tau_{xz}}{\partial x}+\frac{\partial \tau_{yz}}{\partial y}+\frac{\partial \sigma_z}{\partial z}=P_x\frac{\partial^2 w}{\partial x^2}+P_y\frac{\partial^2 w}{\partial y^2}+\rho\omega^2 w \tag{5}$$

The stress–displacement relationships are shown below:

$$\begin{bmatrix}\sigma_x\\ \sigma_y\\ \sigma_z\\ \tau_{yz}\\ \tau_{xz}\\ \tau_{xy}\end{bmatrix}=\begin{bmatrix} C_{11}\frac{\partial}{\partial x} & C_{12}\frac{\partial}{\partial y} & C_{13}\frac{\partial}{\partial z}\\ C_{12}\frac{\partial}{\partial x} & C_{22}\frac{\partial}{\partial y} & C_{23}\frac{\partial}{\partial z}\\ C_{13}\frac{\partial}{\partial x} & C_{23}\frac{\partial}{\partial y} & C_{33}\frac{\partial}{\partial z}\\ 0 & C_{44}\frac{\partial}{\partial z} & C_{44}\frac{\partial}{\partial y}\\ C_{55}\frac{\partial}{\partial z} & 0 & C_{55}\frac{\partial}{\partial x}\\ C_{66}\frac{\partial}{\partial y} & C_{66}\frac{\partial}{\partial x} & \end{bmatrix}\times\begin{bmatrix}u\\ v\\ w\end{bmatrix} \tag{6}$$

In the above equations [eqns (3)–(6)], σ_x, σ_y and σ_z represent the stresses in the x-, y- and z-directions and τ_{xy}, τ_{xz} and τ_{yx} are the shear stresses in the x–y, x–z and the y–z planes. C_{11}, C_{22}, C_{33}, C_{13}, C_{23}, C_{44}, C_{55} and C_{66} are the nine elastic constants for orthotropic materials. The displacements in the x-, y-, and z-directions are represented as u, v, and w, respectively; the angular frequency of vibration is represented by the symbol ω; the density is represented by the symbol ρ. The terms P_x and P_y are the destabilizing loads on the body in the x-, and y-directions, respectively. By substituting eqns (6) into eqns (3)–(5), the equilibrium equations in terms of the displacements (governing equations) can be obtained as follows:

$$C_{11}\frac{\partial^2 u}{\partial x^2}+C_{66}\frac{\partial^2 u}{\partial y^2}+C_{55}\frac{\partial^2 u}{\partial z^2}+(C_{12}+C_{66})\frac{\partial^2 v}{\partial x\,\partial y}+(C_{13}+C_{55})\frac{\partial^2 w}{\partial x\,\partial z}=P_x\left(\frac{\partial^2 u}{\partial x^2}+\phi\frac{\partial^2 u}{\partial y^2}\right)+\rho\omega^2 u \tag{7}$$

$$(C_{12}+C_{66})\frac{\partial^2 u}{\partial x\,\partial y}+C_{66}\frac{\partial^2 v}{\partial x^2}+C_{22}\frac{\partial^2 v}{\partial y^2}+C_{44}\frac{\partial^2 v}{\partial z^2}+(C_{23}+C_{44})\frac{\partial^2 w}{\partial y\,\partial z}=P_x\left(\frac{\partial^2 v}{\partial x^2}+\phi\frac{\partial^2 v}{\partial y^2}\right)+\rho\omega^2 v \tag{8}$$

$$(C_{13}+C_{55})\frac{\partial^2 u}{\partial x\,\partial z}+(C_{23}+C_{44})\frac{\partial^2 v}{\partial y\,\partial z}+C_{55}\frac{\partial^2 w}{\partial x^2}$$
$$+C_{44}\frac{\partial^2 w}{\partial y^2}+C_{33}\frac{\partial^2 w}{\partial z^2}=P_x\left(\frac{\partial^2 w}{\partial x^2}+\phi\frac{\partial^2 w}{\partial y^2}\right)+\rho\omega^2 w \quad (9)$$

The term ϕ in eqns (7)–(9) is the ratio of the destabilizing loads. It is defined as:

$$\phi=\frac{P_y}{\pi_x} \quad (10)$$

3.2. Boundary conditions

For the three-dimensional analysis of a plate, boundary conditions need to be applied to all the six faces. The boundary conditions at the four faces of the plate where $x=0$, a and $y=0$, b are called edge boundary conditions. The boundary conditions at the top and bottom surfaces of the plate where $z=0$, c are called lateral surface boundary conditions. Below are the equations describing the boundary conditions.

3.2.1. Edge boundary conditions

- Simply supported edge boundary conditions (S):

$$\text{At } x=0 \text{ and } a: \quad \sigma_x=0; \quad v=0; \quad w=0 \quad (11a)$$

$$\text{At } y=0 \text{ and } b: \quad \sigma_y=0; \quad u=0; \quad w=0 \quad (11b)$$

- Clamped edge boundary conditions (C):

$$u=0; \quad v=0; \quad w=0 \quad (12)$$

3.2.2. Lateral surface boundary conditions

In this paper, a uniform load q is applied to the top lateral surface of the plate for bending analysis.

- Loading on the top surface:

$$\text{On } z=0: \quad \sigma_z=-q; \quad \tau_{xz}=0; \quad \tau_{yz}=0 \quad (13a)$$

$$\text{On } z=c; \quad \sigma_z=0; \quad \tau_{xz}=0; \quad \tau_{yz}=0 \quad (13b)$$

For buckling and free vibration analyses, the lateral surfaces are considered free.

- Free lateral surface condition:

$$\sigma_z=0; \quad \tau_{xz}=0; \quad \tau_{yz}=0 \quad (14)$$

4. DQ formulations

The DQ procedure for solving a system of partial differential equations is first to normalize the geometry of the plate and then discretize it into grid points according to the directions of the

solution domain. The discretizing process involves applying the DQ approximation to the equilibrium equations and the boundary conditions.

4.1. Normalization

The following non-dimensional parameters are introduced in the normalization process:

$$X = \frac{x}{a}; \quad Y = \frac{y}{b}; \quad Z = \frac{z}{c} \tag{15a–c}$$

$$U = \frac{u}{a}; \quad V = \frac{v}{b}; \quad W = \frac{w}{a} \tag{15d–f}$$

$$\alpha = \frac{a}{b}; \quad \beta = \frac{c}{b}; \quad \gamma = \frac{c}{a} \tag{15g–i}$$

In the above equations [eqns (15)], a, b and c represent the dimensions of the plate in the x-, y- and z-directions, respectively. Substituting eqns (15) into the equilibrium equations [eqns (7)–(9)] results in the following normalized governing equations:

$$\gamma^2 C_{11}\frac{\partial^2 U}{\partial X^2} + \beta^2 C_{66}\frac{\partial^2 U}{\partial Y^2} + C_{55}\frac{\partial^2 U}{\partial Z^2} + \gamma^2(C_{12}+C_{66})\frac{\partial^2 V}{\partial X\,\partial Y} + \gamma(C_{13}+C_{55})\frac{\partial^2 W}{\partial X\,\partial Z} = P_x\left[\gamma^2\frac{\partial^2 U}{\partial X^2} + \phi\beta^2\frac{\partial^2 U}{\partial Y^2}\right] - \rho\omega^2 c^2 U \tag{16}$$

$$\beta^2(C_{12}+C_{66})\frac{\partial^2 U}{\partial X\,\partial Y} + \gamma^2 C_{66}\frac{\partial^2 V}{\partial X^2} + \beta^2 C_{22}\frac{\partial^2 V}{\partial Y^2} + C_{44}\frac{\partial^2 V}{\partial Z^2} + \alpha\beta(C_{23}+C_{44})\frac{\partial^2 W}{\partial Y\,\partial Z} = P_x\left[\gamma^2\frac{\partial^2 V}{\partial X^2} + \phi\beta^2\frac{\partial^2 V}{\partial Y^2}\right] - \rho\omega^2 c^2 V \tag{17}$$

$$\gamma(C_{13}+C_{55})\frac{\partial^2 U}{\partial X\,\partial Z} + \gamma(C_{23}+C_{44})\frac{\partial^2 V}{\partial Y\,\partial Z} + \gamma^2 C_{55}\frac{\partial^2 W}{\partial X^2} + \beta^2 C_{44}\frac{\partial^2 W}{\partial Y^2} + C_{33}\frac{\partial^2 W}{\partial Z^2} = P_x\left[\gamma^2\frac{\partial^2 W}{\partial X^2} + \phi\beta^2\frac{\partial^2 W}{\partial Y^2}\right] - \rho\omega^2 c^2 W \tag{18}$$

By substituting the non-dimensional parameters into the stress displacement equations [eqns (6)] and the boundary conditions [eqns (11)–(14)], one can obtain the following normalised boundary equations:

• Simply supported edge boundary condition (S) for $X = 0$, 1:

$$\gamma\frac{\partial U}{\partial X} + \gamma\frac{C_{12}}{C_{11}}\frac{\partial V}{\partial Y} + \frac{C_{13}}{C_{11}}\frac{\partial W}{\partial Z} = 0 \tag{19a}$$

$$V = 0 \tag{19b}$$

$$W = 0 \tag{19c}$$

• Clamped edge boundary condition (C):

$$U = 0 \tag{20a}$$

$$V = 0 \tag{20b}$$

$$W = 0 \tag{20c}$$

• Loading condition at the top surface:

$$\gamma \frac{C_{13}}{C_{11}} \frac{\partial U}{\partial X} + \gamma \frac{C_{23}}{C_{11}} \frac{\partial V}{\partial Y} + \frac{C_{33}}{C_{11}} \frac{\partial W}{\partial Z} = -\frac{\gamma q}{C_{11}} \tag{21a}$$

$$\gamma \frac{\partial W}{\partial X} + \frac{\partial U}{\partial Z} = 0 \tag{21b}$$

$$\frac{\partial V}{\partial Z} + \alpha\beta \frac{\partial W}{\partial Y} = 0 \tag{21c}$$

• Free lateral surface condition:

$$\gamma \frac{C_{13}}{C_{11}} \frac{\partial U}{\partial X} + \gamma \frac{C_{23}}{C_{11}} \frac{\partial V}{\partial Y} + \frac{C_{33}}{C_{11}} \frac{\partial W}{\partial Z} = 0 \tag{22a}$$

$$\gamma \frac{\partial W}{\partial X} + \frac{\partial U}{\partial Z} = 0 \tag{22b}$$

$$\frac{\partial V}{\partial Z} + \alpha\beta \frac{\partial W}{\partial Y} = 0 \tag{22c}$$

4.2. Discretization

According to the differential quadrature procedure, the normalized governing equations [eqns (16)–(18)] can be discretized into the following form:

$$\begin{aligned} &\gamma^2 C_{11} \sum_{l=1}^{N_X} A_{il}^{(2)} U_{ljk} + \beta^2 C_{66} \sum_{m=1}^{N_Y} B_{jm}^{(2)} U_{imk} + C_{55} \sum_{n=1}^{N_Z} C_{kn}^{(2)} U_{ijn} \\ &\quad + \gamma^2 (C_{12} + C_{66}) \sum_{l=1}^{N_X} A_{il}^{(1)} \sum_{m=1}^{N_Y} B_{jm}^{(1)} V_{lmk} + \gamma (C_{13} + C_{55}) \sum_{l=1}^{N_X} A_{il}^{(1)} \sum_{n=1}^{N_Z} C_{kn}^{(1)} W_{ljn} \\ &\quad = P_X \left[\gamma^2 \sum_{l=1}^{N_X} A_{il}^{(2)} U_{ljk} + \phi\beta^2 \sum_{m=1}^{N_Y} B_{jm}^{(2)} U_{imk} \right] - \rho\omega^2 c^2 U_{ijk} \end{aligned} \tag{23}$$

$$\beta^2(C_{12}+C_{66})\sum_{l=1}^{N_X}A_{il}^{(1)}\sum_{m=1}^{N_Y}B_{jm}^{(1)}U_{lmk}+\gamma^2C_{66}\sum_{l=1}^{N_X}A_{il}^{(2)}V_{ljk}+\beta^2C_{22}\sum_{m=1}^{N_Y}B_{jm}^{(2)}V_{imk}$$
$$+C_{44}\sum_{n=1}^{N_\beta}C_{kn}^{(2)}V_{ijn}+\alpha\beta(C_{23}+C_{44})\sum_{m=1}^{N_Y}B_{jm}^{(1)}\sum_{n=1}^{N_Z}C_{kn}^{(1)}W_{imn}$$
$$=P_x\left[\gamma^2\sum_{l=1}^{N_X}A_{il}^{(2)}V_{ljk}+\phi\beta^2\sum_{m=1}^{N_Y}B_{jm}^{(2)}V_{imk}\right]-\rho\omega^2c^2V_{ijk} \tag{24}$$

$$\gamma(C_{13}+C_{55})\sum_{l=1}^{N_X}A_{il}^{(1)}\sum_{n=1}^{N_Z}C_{kn}^{(1)}U_{ljn}+\gamma(C_{23}+C_{44})\sum_{m=1}^{N_Y}B_{jm}^{(1)}\sum_{n=1}^{N_Z}C_{kn}^{(1)}V_{imn}$$
$$+\gamma^2C_{55}\sum_{l=1}^{N_X}A_{il}^{(2)}W_{ijk}+\beta^2C_{44}\sum_{m=1}^{N_Y}B_{jm}^{(2)}W_{imk}+C_{33}\sum_{n=1}^{N_Z}C_{kn}^{(2)}W_{ijn}$$
$$=P_x\left[\gamma^2\sum_{l=1}^{N_X}A_{il}^{(2)}W_{ljk}+\phi\beta^2\sum_{m=1}^{N_Y}B_{jm}^{(2)}W_{imk}\right]-\rho\omega^2c^2W_{ijk} \tag{25}$$

Similarly, the differential quadrature procedure is applied to the normalized boundary conditions [eqns (19)–(22)]. These equations are discretized as follows:

• Simply supported edge boundary condition (S) for $X=0$, 1:

$$\gamma\sum_{l=1}^{N_X}A_{il}^{(1)}U_{ljk}+\gamma\frac{C_{12}}{C_{11}}\sum_{m=1}^{N_Y}B_{jm}^{(1)}V_{imk}+\frac{C_{13}}{C_{11}}\sum_{n=1}^{N_Z}C_{kn}^{(1)}W_{ijn}=0 \tag{26a}$$

$$V_{ijk}=0 \tag{26b}$$

$$W_{ijk}=0 \tag{26c}$$

• Clamped edge boundary condition (C):

$$U_{ijk}=0 \tag{27a}$$

$$V_{ijk}=0 \tag{27b}$$

$$W_{ijk}=0 \tag{27c}$$

• Loading condition at the top surface:

$$\gamma\frac{C_{13}}{C_{11}}\sum_{l=1}^{N_X}A_{il}^{(1)}U_{ljk}+\gamma\frac{C_{23}}{C_{11}}\sum_{m=1}^{N_Y}B_{jm}^{(1)}V_{imk}+\frac{C_{33}}{C_{11}}\sum_{n=1}^{N_Z}C_{kn}^{(1)}W_{ijn}=\frac{-q\gamma}{C_{11}} \tag{28a}$$

$$\sum_{n=1}^{N_Z}C_{kn}^{(1)}U_{ijn}+\gamma\sum_{l=1}^{N_X}A_{il}^{(1)}W_{ljk}=0 \tag{28b}$$

$$\sum_{n=1}^{N_Z} C_{kn}^{(1)} V_{ijn} + \alpha\beta \sum_{m=1}^{N_Y} B_{jm}^{(1)} W_{imk} = \quad 0 \tag{28c}$$

• Free lateral surface condition:

$$\gamma \frac{C_{13}}{C_{11}} \sum_{l=1}^{N_X} A_{il}^{(1)} U_{ljk} + \gamma \frac{C_{23}}{C_{11}} \sum_{m=1}^{N_Y} B_{jm}^{(1)} V_{imk} + \frac{C_{33}}{C_{11}} \sum_{n=1}^{N_Z} C_{kn}^{(1)} W_{ijn} = 0 \tag{29a}$$

$$\gamma \sum_{l=1}^{N_X} A_{il}^{(1)} W_{ljk} + \sum_{n=1}^{N_Z} C_{kn}^{(1)} U_{ijn} = 0 \tag{29b}$$

$$\sum_{n=1}^{N_Z} C_{kn}^{(1)} V_{ijn} + \alpha\beta \sum_{m=1}^{N_Y} B_{jm}^{(1)} W_{imk} = 0 \tag{29c}$$

5. Method of solution

For bending analysis, the terms P_x, P_y, and ω in eqns (3)–(5) are set to zero. Hence, the resulting discretized governing equations for bending analysis become:

$$\gamma^2 C_{11} \sum_{l=1}^{N_X} A_{il}^{(2)} U_{ljk} + \beta^2 C_{66} \sum_{m=1}^{N_Y} B_{jm}^{(2)} U_{imk} + C_{55} \sum_{n=1}^{N_Z} C_{kn}^{(2)} U_{ijn} + \gamma^2 (C_{12} + C_{66}) \sum_{l=1}^{N_X} A_{il}^{(1)} \sum_{m=1}^{N_Y} B_{jm}^{(1)} V_{lmk} + \gamma (C_{13} + C_{55}) \sum_{l=1}^{N_X} A_{il}^{(1)} \sum_{n=1}^{N_Z} C_{kn}^{(1)} W_{ljn} = 0 \tag{30}$$

$$\beta^2 (C_{12} + C_{66}) \sum_{l=1}^{N_X} A_{il}^{(1)} \sum_{m=1}^{N_Y} B_{jm}^{(1)} U_{lmk} + \gamma^2 C_{66} \sum_{l=1}^{N_X} A_{il}^{(2)} V_{ljk} + \beta^2 C_{22} \sum_{m=1}^{N_Y} B_{jm}^{(2)} V_{imk} + C_{44} \sum_{n=1}^{N_Z} C_{kn}^{(2)} V_{ijn} + \alpha\beta (C_{23} + C_{44}) \sum_{m=1}^{N_Y} B_{jm}^{(1)} \sum_{n=1}^{N_Z} C_{kn}^{(1)} W_{imn} = 0 \tag{31}$$

$$\gamma (C_{13} + C_{55}) \sum_{l=1}^{N_X} A_{il}^{(1)} \sum_{n=1}^{N_Z} C_{kn}^{(1)} U_{ljn} + \gamma (C_{23} + C_{44}) \sum_{m=1}^{N_Y} B_{jm}^{(1)} \sum_{n=1}^{N_Z} C_{kn}^{(1)} V_{imn} + \gamma^2 C_{55} \sum_{l=1}^{N_X} A_{il}^{(2)} W_{ljk} + \beta^2 C_{44} \sum_{m=1}^{N_Y} B_{jm}^{(2)} W_{imk} + C_{33} \sum_{n=1}^{N_Z} C_{kn}^{(2)} W_{ijn} = 0 \tag{32}$$

For buckling analysis, the term ω in eqns (3)–(5) is ignored. Hence, the resulting discretized governing equations for buckling analysis become:

$$\gamma^2 C_{11} \sum_{l=1}^{N_X} A_{il}^{(2)} U_{ljk} + \beta^2 C_{66} \sum_{m=1}^{N_Y} B_{jm}^{(2)} U_{imk} + C_{55} \sum_{n=1}^{N_Z} C_{kn}^{(2)} U_{ijn}$$
$$+ \gamma^2 (C_{12} + C_{66}) \sum_{l=1}^{N_X} A_{il}^{(1)} \sum_{m=1}^{N_Y} B_{jm}^{(1)} V_{lmk} + \gamma (C_{13} + C_{55}) \sum_{l=1}^{N_X} A_{il}^{(1)} \sum_{n=1}^{N_Z} C_{kn}^{(1)} W_{ljn}$$
$$= P_x \left[\gamma^2 \sum_{l=1}^{N_X} A_{il}^{(2)} U_{ljk} + \phi \beta^2 \sum_{m=1}^{N_Y} B_{jm}^{(2)} U_{imk} \right] \tag{33}$$

$$\beta^2 (C_{12} + C_{66}) \sum_{l=1}^{N_X} A_{il}^{(1)} \sum_{m=1}^{N_Y} B_{jm}^{(1)} U_{lmk} + \gamma^2 C_{66} \sum_{l=1}^{N_X} A_{il}^{(2)} V_{ljk} + \beta^2 C_{22} \sum_{m=1}^{N_Y} B_{jm}^{(2)} V_{imk}$$
$$+ C_{44} \sum_{n=1}^{N_Z} C_{kn}^{(2)} V_{ijn} + \alpha \beta (C_{23} + C_{44}) \sum_{m=1}^{N_Y} B_{jm}^{(1)} \sum_{n=1}^{N_Z} C_{kn}^{(1)} W_{imn}$$
$$= P_x \left[\gamma^2 \sum_{l=1}^{N_X} A_{il}^{(2)} V_{ljk} + \phi \beta^2 \sum_{m=1}^{N_Y} B_{jm}^{(2)} V_{imk} \right] \tag{34}$$

$$\gamma (C_{13} + C_{55}) \sum_{l=1}^{N_X} A_{il}^{(1)} \sum_{n=1}^{N_Z} C_{kn}^{(1)} U_{ljn} + \gamma (C_{23} + C_{44}) \sum_{m=1}^{N_Y} B_{jm}^{(1)} \sum_{n=1}^{N_Z} C_{kn}^{(1)} V_{imn}$$
$$+ \gamma^2 C_{55} \sum_{l=1}^{N_X} A_{il}^{(2)} W_{ljk} + \beta^2 C_{44} \sum_{m=1}^{N_Y} B_{jm}^{(2)} W_{imk} + C_{33} \sum_{n=1}^{N_Z} C_{kn}^{(2)} W_{ijn}$$
$$= P_x \left[\gamma^2 \sum_{l=1}^{N_X} A_{il}^{(2)} W_{ljk} + \phi \beta^2 \sum_{m=1}^{N_Y} B_{jm}^{(2)} W_{imk} \right] \tag{35}$$

For free vibration analysis, the terms P_x, P_y in eqns (3)–(5) are set to zero. Hence, the resulting discretized governing equations for free vibration analysis become:

$$\gamma^2 C_{11} \sum_{l=1}^{N_X} A_{il}^{(2)} U_{ljk} + \beta^2 C_{66} \sum_{m=1}^{N_Y} B_{jm}^{(2)} U_{imk} + C_{55} \sum_{n=1}^{N_Z} C_{kn}^{(2)} U_{ijn}$$
$$+ \gamma^2 (C_{12} + C_{66}) \sum_{l=1}^{N_X} A_{il}^{(1)} \sum_{m=1}^{N_Y} B_{jm}^{(1)} V_{lmk} + \gamma (C_{13} + C_{55}) \sum_{l=1}^{N_X} A_{il}^{(1)} \sum_{n=1}^{N_Z} C_{kn}^{(1)} W_{ljn} = -\rho \omega^2 c^2 U_{ijk} \tag{36}$$

$$\beta^2 (C_{12} + C_{66}) \sum_{l=1}^{N_X} A_{il}^{(1)} \sum_{m=1}^{N_Y} B_{jm}^{(1)} U_{lmk} + \gamma^2 C_{66} \sum_{l=1}^{N_X} A_{il}^{(2)} V_{ljk} + \beta^2 C_{22} \sum_{m=1}^{N_Y} B_{jm}^{(2)} V_{imk}$$
$$+ C_{44} \sum_{n=1}^{N_Z} C_{kn}^{(2)} V_{ijn} + \alpha \beta (C_{23} + C_{44}) \sum_{m=1}^{N_Y} B_{jm}^{(1)} \sum_{n=1}^{N_Z} C_{kn}^{(1)} W_{imn} = -\rho \omega^2 c^2 V_{ijk} \tag{37}$$

$$\gamma(C_{13}+C_{55})\sum_{l=1}^{N_X}A_{il}^{(1)}\sum_{n=1}^{N_Z}C_{kn}^{(1)}U_{ljn}+\gamma(C_{23}+C_{44})\sum_{m=1}^{N_Y}B_{jm}^{(1)}\sum_{n=1}^{N_Z}C_{kn}^{(1)}V_{imn}$$

$$+\gamma^2C_{55}\sum_{l=1}^{N_X}A_{il}^{(2)}W_{ljk}+\beta^2C_{44}\sum_{m=1}^{N_Y}B_{jm}^{(2)}W_{imk}+C_{33}\sum_{n=1}^{N_Z}C_{kn}^{(2)}W_{ijn}=-\rho\omega^2c^2W_{ijk} \quad (38)$$

The determinant of the matrix to be solved for a solution domain with a grid size of $N_x \times N_y \times N_z$ is $(3 \times N_x \times N_y \times N_z)$, because for every point in the solution domain there are three conditions that need to be satisfied, i.e., the three governing equations or the three equations describing the boundary condition under consideration.

The points on the lateral surface of the plate are described by either the loading condition (for bending analysis) or the free lateral surface boundary (for the buckling and free vibration analyses). The points along the edges of the plate are described by the respective edge boundary conditions.

The grid pattern used in this study is determined by the following function:

$$\Theta(i)=\frac{1}{2}\left(1-\cos\frac{(i-1)\pi}{N-1}\right) \quad (39)$$

In eqn (39), $\Theta(i)$ can be the $x(i)$, $y(i)$ or $z(i)$ co-ordinate of the ith points considered.

In this study, the programming language used is FORTRAN 77. The computation is implemented using a Digital Alpha Server 8400 5/440 system.

6. Results and discussion

The orthotropic material used for the implementation of the DQ solution corresponds to the properties of the Aragonite crystal (Bisplinghoff et al., 1965) shown in Table 1.

In presenting the solution for the bending of an orthotropic plate, the non-dimensional parameters used for deflection, stress in the x-direction, and stress in the y-direction are $C_{11}w/cq$, σ_x/q, and σ_y/q, respectively. For buckling analysis, the non-dimensional buckling factor, k, is defined as

$$k=P_x\gamma^2\pi^2/C_{11} \quad (40)$$

For free vibration analysis, the non-dimensional frequency parameter, λ, is defined as

$$\lambda=\omega\sqrt{\rho c^2/C_{11}} \quad (41)$$

Table 1
Properties of Aragonite crystal

$C_{22}/C_{11}=0.543103$	$C_{33}/C_{11}=0.530172$
$C_{12}/C_{11}=0.23319$	$C_{13}/C_{11}=0.010776$
$C_{23}/C_{11}=0.098276$	$C_{66}/C_{11}=0.262931$
$C_{55}/C_{11}=0.159914$	$C_{44}/C_{11}=0.26681$

To clarify the notation used to describe the boundary conditions, we shall use the SCSC plate as an example. The description 'SCSC' means the plate has sides $X = 0$ and $X = 1$ simply supported and the sides $Y = 0$ and $Y = 1$ clamped.

Since this present method of calculating the weighting coefficients rids the ill-conditioning problems, the authors hence decided to calculate the results presented in this paper till a maximum grid size of $13 \times 13 \times 13$. It is deduced that the result will not be worst off even when more grid points are used.

6.1. Bending analysis

Tables 2–4 show the convergence and accuracy studies of the deflections, and stresses of a homogeneous SSSS orthotropic plate with aspect ratios of 0.5, 1.0 and 2.0, respectively. The

Table 2
Convergence and accuracy studies of deflections and stresses in homogeneous SSSS orthotropic plates ($a/b = 0.5$) under uniform surface load

c/a	Grid size	$C_{11}w/cq$ ($X = Y = Z = 0.5$)	σ_x/q ($X = 0$, $Y = Z = 0.5$)	σ_y/q ($X = 0$, $Y = Z = 0.5$)
0.05	$5 \times 5 \times 5$	−21,924.8	274.317	94.3799
	$7 \times 7 \times 7$	−21,407.2	260.562	77.3116
	$9 \times 9 \times 9$	−21,542.4	262.656	79.6751
	$11 \times 11 \times 11$	−21,542.5	262.671	79.5721
	$13 \times 13 \times 13$	−21,542.3	262.687	79.5362
	Exact solution[1]	−21,542.0	262.67	79.545
	Reissner's theory[1]	−21,542.0	262.07	79.337
	Classical plate theory[1]	−21,201.0	262.26	79.121
0.10	$5 \times 5 \times 5$	−1435.66	68.9771	24.0100
	$7 \times 7 \times 7$	−1399.88	65.3930	19.6352
	$9 \times 9 \times 9$	−1408.48	66.0219	20.2404
	$11 \times 11 \times 11$	−1408.51	65.9385	20.2050
	$13 \times 13 \times 13$	−1408.48	66.0122	20.2122
	Exact solution[1]	−1408.5	65.975	20.204
	Reissner's theory[1]	−1408.4	65.379	20.001
	Classical plate theory[1]	−1325.1	65.564	19.780
0.14	$5 \times 5 \times 5$	−395.419	35.4730	12.5246
	$7 \times 7 \times 7$	−384.968	33.5253	10.2163
	$9 \times 9 \times 9$	−387.244	33.9277	10.5426
	$11 \times 11 \times 11$	−387.257	33.8135	10.5054
	$13 \times 13 \times 13$	−387.248	33.9035	10.5314
	Exact solution[1]	−387.23	33.862	10.515
	Reissner's theory[1]	−387.27	33.265	10.312
	Classical plate theory[1]	−344.93	33.451	10.092

[1] Srinivas and Rao (1970).

Table 3
Convergence and accuracy studies of deflections and stresses in homogeneous SSSS orthotropic plates ($a/b = 1.0$) under uniform surface load

c/a	Grid size	$C_{11}w/cq$ ($X = Y = Z = 0.5$)	σ_x/q ($X = 0$, $Y = Z = 0.5$)	σ_y/q ($X = 0$, $Y = Z = 0.5$)
0.05	$5 \times 5 \times 5$	−10,174.6	147.423	91.1932
	$7 \times 7 \times 7$	−10,426.7	144.115	86.9235
	$9 \times 9 \times 9$	−10,443.3	144.328	87.0700
	$11 \times 11 \times 11$	−10,443.5	144.285	87.0825
	$13 \times 13 \times 13$	−10,443.5	144.339	87.0900
	Exact solution[1]	−10,443.0	144.31	87.080
	Reissner's theory[1]	−10,442.0	143.87	86.921
	Classical plate theory[1]	−10,246.0	144.39	86.487
0.10	$5 \times 5 \times 5$	−673.563	36.9578	23.3322
	$7 \times 7 \times 7$	−687.561	35.9110	22.1651
	$9 \times 9 \times 9$	−688.659	36.0766	22.2311
	$11 \times 11 \times 11$	−688.633	35.9740	22.1908
	$13 \times 13 \times 13$	−688.626	36.0652	22.2334
	Exact solution[1]	−688.57	36.021	22.210
	Reissner's theory[1]	−688.37	35.578	22.048
	Classical plate theory[1]	−640.39	36.098	21.622
0.14	$5 \times 5 \times 5$	−187.741	18.9416	12.2516
	$7 \times 7 \times 7$	−190.818	18.2391	11.5769
	$9 \times 9 \times 9$	−191.119	18.4213	11.6522
	$11 \times 11 \times 11$	−191.096	18.2900	11.5852
	$13 \times 13 \times 13$	−191.094	18.3914	11.6389
	Exact solution[1]	−191.07	18.346	11.615
	Reissner's theory[1]	−191.02	17.906	11.453
	Classical plate theory[1]	−166.70	18.417	11.031

[1] Srinivas and Rao (1970).

thickness to length ratios of the plate, c/a, considered in these tables are 0.05, 0.10 and 0.14. The tables also show solutions from classical plate theory, first-order shear deformation plate theory and three-dimensional elasticity theory. For comparison purposes, the exact solution of Srinivas and Rao (1970) is chosen as the benchmark here.

From the tables, one can observe that for the deflection of an orthotropic plate with thickness to length ratios of 0.05 and 0.1, convergence of up to five significant figures can be reached at a grid size of $11 \times 11 \times 11$. When the plate has a thickness to length ratio of 0.14, converged results with a minimum of three significant figures can be reached at a grid size of $9 \times 9 \times 9$.

When the DQ solutions for central deflection are compared with the exact solution (Srinivas and Rao, 1970), one may observe that, for plates with thickness to length ratio of 0.05 and 0.1, accuracy to five significant figures is obtained at a grid size of $13 \times 13 \times 13$. For plates with thickness to length ratio of 0.14, the deflection reaches four significant figures accuracy at a grid size of

Table 4
Convergence and accuracy studies of deflections and stresses in homogeneous SSSS orthotropic plates ($a/b = 2.0$) under uniform surface load

c/a	Grid size	$C_{11}w/cq$ ($X = Y = Z = 0.5$)	σ_x/q ($X = 0$, $Y = Z = 0.5$)	σ_y/q ($X = 0$, $Y = Z = 0.5$)
0.05	$5 \times 5 \times 5$	−2028.76	45.2020	55.4610
	$7 \times 7 \times 7$	−2043.00	40.2061	54.1016
	$9 \times 9 \times 9$	−2048.98	40.7001	54.2995
	$11 \times 11 \times 11$	−2048.90	40.6312	54.2696
	$13 \times 13 \times 13$	−2048.89	40.6918	54.3026
	Exact solution[1]	−2048.7	40.657	54.279
	Reissner's theory[1]	−2047.9	40.477	54.134
	Classical plate theory[1]	−1988.1	40.860	53.838
0.10	$5 \times 5 \times 5$	−138.554	11.2072	14.2526
	$7 \times 7 \times 7$	−138.769	9.84381	13.8122
	$9 \times 9 \times 9$	−139.147	10.0996	13.9419
	$11 \times 11 \times 11$	−139.095	9.97419	13.8588
	$13 \times 13 \times 13$	−139.099	10.0680	13.9116
	Exact solution[1]	−139.08	10.025	13.888
	Reissner's theory[1]	−138.93	9.8460	13.743
	Classical plate theory[1]	−124.26	10.215	13.460
0.14	$5 \times 5 \times 5$	−39.8873	5.69865	7.53636
	$7 \times 7 \times 7$	−39.7154	4.88041	7.19866
	$9 \times 9 \times 9$	−39.8187	5.12394	7.33862
	$11 \times 11 \times 11$	−39.7932	4.97958	7.24854
	$13 \times 13 \times 13$	−39.7976	5.08019	7.30263
	Exact solution[1]	−39.790	5.0364	7.7294
	Reissner's theory[1]	−39.753	4.8603	7.1358
	Classical plate theory[1]	−32.345	5.2118	6.8671

[1] Srinivas and Rao (1970).

$13 \times 13 \times 13$ for plate aspect ratios of 0.5 and 1.0. For a plate aspect ratio of 2.0, three significant figures accuracy is reached at a similar grid size.

The mid-surface deflection converges to at least two significant figures at a grid size of $11 \times 11 \times 11$. When compared with the exact solution (Srinivas and Rao, 1970), the DQ solution has less than 3% error when the grid size of $9 \times 9 \times 9$ and above are used.

It should also be commented that the convergence pattern for the deflection of the SSSS plates is monotonic whereas the convergence pattern for the deflection of the SCSC plate is oscillatory. For the convergence of the stresses, one can generally conclude that the convergence is oscillatory.

In addition to the above convergence and accuracy studies, some DQ solutions of a SCSC square plate are presented in Table 5. The formula used to calculate successive percentage convergence can be expressed as:

Table 5
Convergence of deflections and stresses in homogeneous SCSC square orthotropic plates under uniform surface load

c/a	Grid size	$C_{11}w/cq$ ($X = Y = Z = 0.5$)	σ_x/q ($X = 0$, $Y = Z = 0.5$)	σ_y/q ($X = 0$, $Y = Z = 0.5$)
0.1	$5\times5\times5$	−416.26	25.040	20.201
	$7\times7\times7$	−403.97	22.059	17.688
	$9\times9\times9$	−404.50	22.186	17.657
	$11\times11\times11$	−404.67	22.015	17.467
	$13\times13\times13$	−404.89	22.223	17.756
0.2	$5\times5\times5$	−34.172	6.6550	5.4631
	$7\times7\times7$	−33.346	5.6559	4.6278
	$9\times9\times9$	−33.463	5.9694	4.9249
	$11\times11\times11$	−33.432	5.7329	4.6521
	$13\times13\times13$	−33.462	5.8968	4.8400
0.3	$5\times5\times5$	−9.3567	3.3565	2.7976
	$7\times7\times7$	−9.0779	2.5725	2.1407
	$9\times9\times9$	−9.1191	2.9151	2.4715
	$11\times11\times11$	−9.1071	2.6999	2.2578
	$13\times13\times13$	−9.1154	2.8396	2.3927
0.4	$5\times5\times5$	−4.0791	2.2784	1.9242
	$7\times7\times7$	−3.9198	1.4982	1.2678
	$9\times9\times9$	−3.9388	1.8546	1.5961
	$11\times11\times11$	−3.9328	1.6422	1.4032
	$13\times13\times13$	−3.9357	1.7803	1.5284
0.5	$5\times5\times5$	−2.2374	1.8454	1.5746
	$7\times7\times7$	−2.1281	1.0149	0.8767
	$9\times9\times9$	−2.1386	1.3975	1.2150
	$11\times11\times11$	−2.1353	1.1714	1.0163
	$13\times13\times13$	−2.1364	1.3181	1.1471

$$\%\ \text{converge}|_{i\times i\times i} = \left|\frac{\text{Solution at } (i\times i\times i) - \text{Solution at } (i-1)\times(i-1)\times(i-1)}{\text{Solution at } (i\times i\times i)}\right| \times 100 \qquad (42)$$

where $i\times i\times i$ is the grid size for which convergence is desired.

Using eqn (42), one can deduce that the worst successive percentage convergence for the SCSC plate's cental deflection is 0.091% at a grid size of $13\times13\times13$. The difference between the successive convergence percentages at grid size $13\times13\times13$ and $11\times11\times11$ is 0.103%. From these results, one can conclude that the DQ solution for deflection of orthotropic plates converges. Contrary to the above favourable findings, percentage convergence for the stresses in x- and y-directions does not seem to be that promising. The percentage convergence at a grid size of $13\times13\times13$ for plates with thickness to length ratios of 0.1, 0.2, 0.3, 0.4 and 0.5 are 1.628, 3.882,

5.638, 8.196 and 11.403%. As observed, convergence gets poorer as the plate thickness to length ratio increases. It is deduced that, in order to obtain acceptable convergence for the stresses in x- and y-directions, we should increase the number of grid points in the solution domain.

6.2. Buckling analysis

The example chosen for convergence and accuracy studies is a SSSS plate. Figures 1 and 2 show convergence of the buckling load for different grid sizes relative to the exact three-dimensional solution by Srinivas and Rao (1970). In these figures, plots with varying thickness to length ratio ranging from 0.1–0.5 are given. From Figs 1 and 2, one can see that the DQ method is able to produce accurate results even at a grid size as small as $8 \times 8 \times 8$. After this grid size, the convergence pattern for all the cases presented is monotonic.

Figures 3 and 4 prevent design curves for buckling factor versus aspect ratio of SSSS and CCCC orthotropic plates. These figures show buckling curves for uniaxially ($\phi = 0$) and biaxially ($\phi = 1.0$) loaded plates. From Fig. 3, it is observed that there is a mode shift from a lower mode to a higher one as the aspect ratio increases for the case of the uniaxially loaded SSSS orthotropic

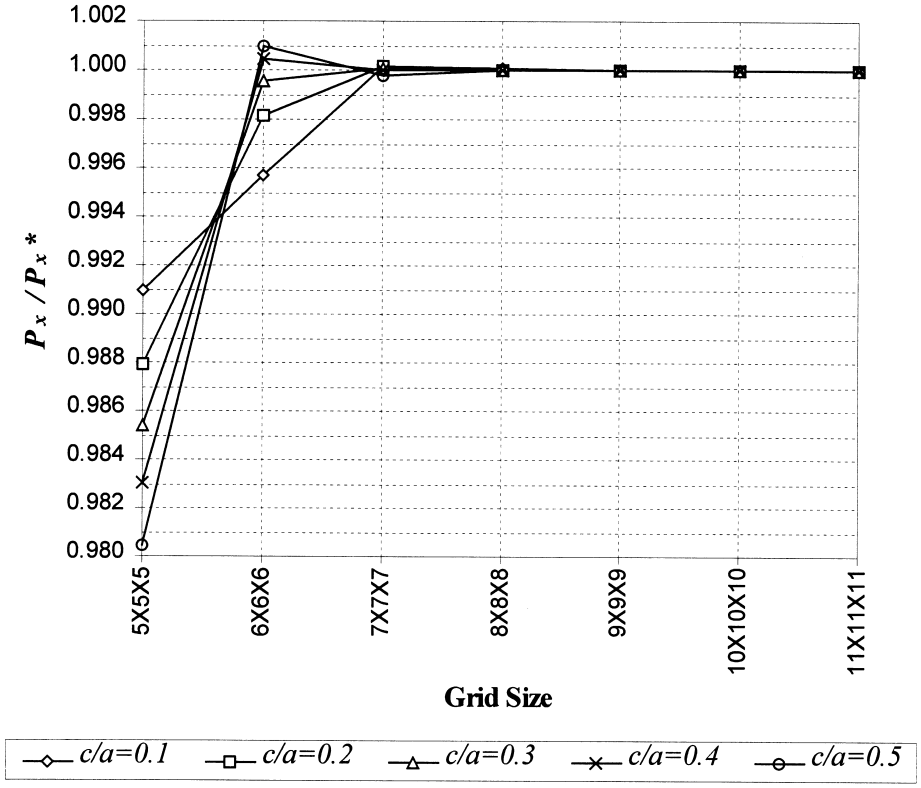

Fig. 1. Convergence and accuracy studies of the buckling factor for an orthotropic SSSS plate with thickness to width ratio, $c/b = 0.1$. [P_x, DQ solution; P_x^*, exact solution, Srinivas and Rao (1970)].

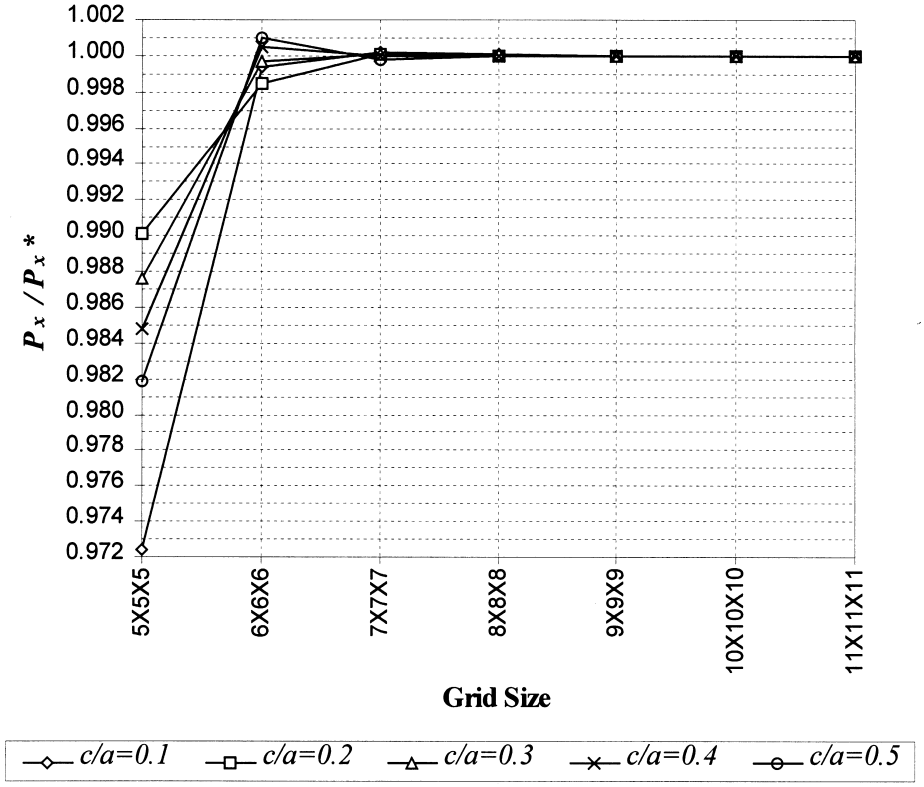

Fig. 2. Convergence and accuracy studies of the buckling factor for an orthotropic SSSS plate with thickness to width ratio, $c/b = 0.2$. [P_x, DQ solution; P_x^*, exact solution, Srinivas and Rao (1970)].

plate. The buckling factor for the biaxially loaded SSSS orthotropic plate decreases as the plate aspect ratio increases. It is also evident that, if the plate thickness to width ratio is kept constant, the buckling factor for the biaxially loaded plate is smaller than that of the uniaxially loaded plate regardless of the plate aspect ratio.

From Fig. 4, one can see that the buckling factor for the CCCC plate decreases as the plate aspect ratio increases. It is also observed that, similar to the SSSS plate, the buckling factor for the uniaxially loaded plate is higher than that for the biaxially loaded plate regardless of the plate aspect ratio. When looking at the graphs for the biaxially loaded plate, one needs to keep in mind that this graph shows the buckling factor expressed in terms of P_x, while the buckling of a biaxially loaded plate is caused by both P_x and P_y.

6.3. Free vibration analysis

Tables 6–9 tabulate the convergence studies for the first eight modes of SSSS, CCCC, SCCC and CSSS plates, respectively. Three thickness to width ratios are considered in this study, i.e., 0.1, 0.3 and 0.5. From the tables, one may observe that a grid size of $10 \times 10 \times 10$ is sufficient to furnish

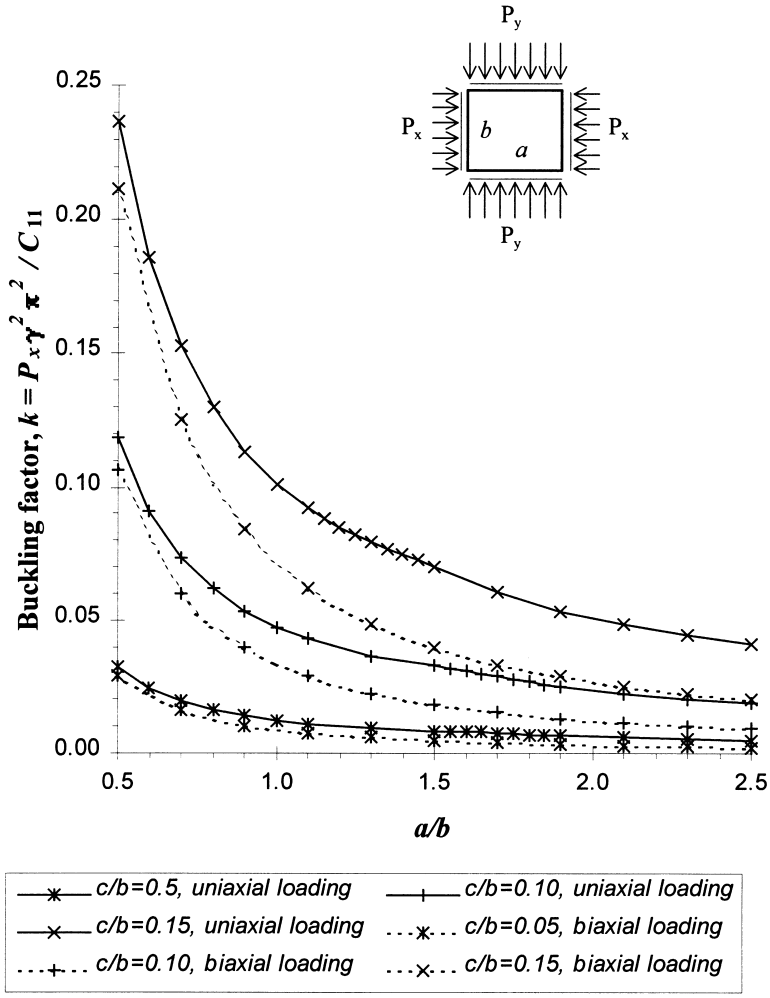

Fig. 3. Buckling factor, $k = P_x\gamma^2\pi^2/C_{11}$, vs aspect ratio, a/b, for SSSS orthotropic plates.

converged results up to three significant figures. From the results, one cannot conclude whether the convergence of the DQ solution is monotonic or oscillatory. The convergence characteristics as deduced from the results changes when different plate thickness and/or boundary conditions are used.

For all eight modes presented for the SSSS plate (Table 6), the successive percentage convergence at a grid size of $11 \times 11 \times 11$ when the plate thickness to width ratios are 0.1, 0.3 and 0.5, is 0.223, 0.003 and 0.008%, respectively. For the CCCC plate (Table 7), the successive percentage convergence at a grid size of $11 \times 11 \times 11$ when the plate thickness to width ratios are 0.1, 0.3 and 0.5, is 0.138, 0.038 and 0.038%, respectively. For the SCCC plate (Table 8), the successive percentage convergence at a grid size of $11 \times 11 \times 11$, when the plate thickness to width ratios are

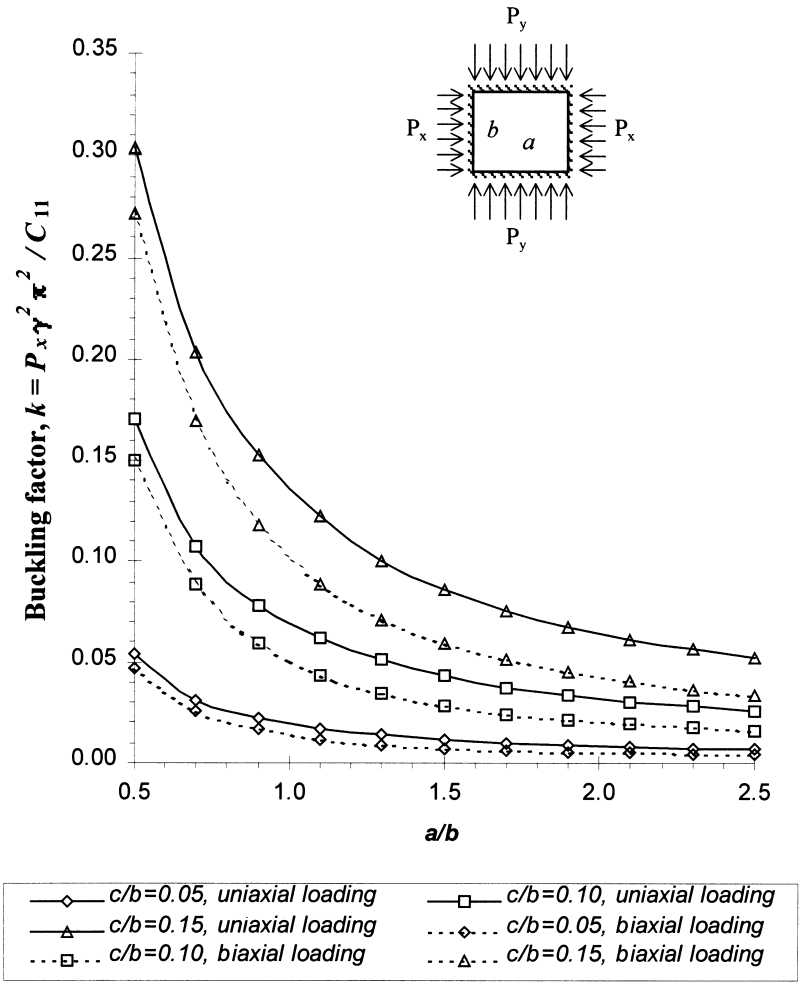

Fig. 4. Buckling factor, $k = P_x\gamma^2\pi^2/C_{11}$, vs aspect ratio, a/b, for CCCC orthotropic plates.

0.1, 0.3 and 0.5, is 0.148, 0.039 and 0.014%, respectively. Finally, for the CSSS plate (Table 9), the successive percentage convergence at a grid size of $11 \times 11 \times 11$,when the plate thickness to width ratios are 0.1, 0.3 and 0.5, is 0.226, 0.011 and 0.006%, respectively. From these observations, one may conclude that the DQ solutions at that grid size have reached convergence.

The next study is to verify the DQ solutions and determine their accuracy. First, the DQ solutions are normalized relatively to the exact solutions by Srinivas and Rao (1970). The normalized frequency parameters are then plotted against the grid sizes. From Fig. 5, one may conclude that the DQ solutions are both accurate and convergent. For this case, an acceptable converged solution starts at a grid size of $8 \times 8 \times 8$.

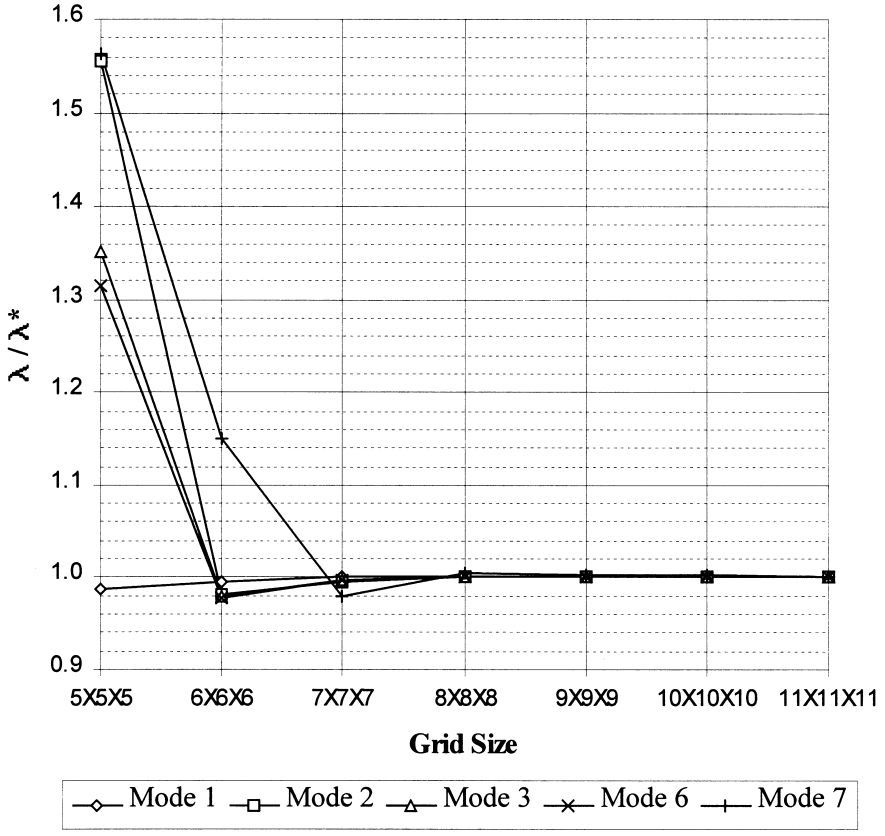

Fig. 5. Convergence and accuracy study of the DQ frequency parameter for a square orthotropic SSSS plate with thickness to width ratio, $c/b = 0.1$, [λ, DQ solution; λ^*, exact 3-D solution by Srinivas and Rao (1970)].

7. Concluding remarks

This paper explored the potential application of the DQ method to three-dimensional bending, buckling and free vibration analyses of orthotropic plates. The details of the DQ formulations were shown and the solution method was detailed. Numerous examples were employed to study the convergence characteristics and the accuracy of the DQ method. The examples showed that a relative coarse grid is sufficient to furnish converged and accurate results. It is, hence, verified that the DQ solutions are correct for the cases studied, and that the method is applicable to the analysis of three-dimensional orthotropic plates.

Table 6
Convergence of frequency parameters, $\lambda = \omega\sqrt{\rho c^2/C_{11}}$ of SSSS square orthotropic plates

		Mode sequence number							
c/b	Grid size X × Y × Z	1	2	3	4	5	6	7	8
0.10	5 × 5 × 5	0.04682	0.16072	0.16072	0.18850	0.21328	0.22292	0.29513	0.34553
	6 × 6 × 6	0.04720	0.10129	0.11639	0.16107	0.16107	0.16547	0.21703	0.31775
	7 × 7 × 7	0.04743	0.10271	0.11839	0.16109	0.16109	0.16886	0.18478	0.21288
	8 × 8 × 8	0.04742	0.10341	0.11895	0.16109	0.16109	0.16957	0.18966	0.21697
	9 × 9 × 9	0.04742	0.10336	0.11884	0.16109	0.16109	0.16948	0.18950	0.21697
	10 × 10 × 10	0.04742	0.10329	0.11880	0.16109	0.16109	0.16941	0.18918	0.21697
	11 × 11 × 11	0.04742	0.10329	0.11880	0.16109	0.16109	0.16941	0.18876	0.21697
Exact Solution[1]		0.0474	0.1033	0.1188	∼	∼	0.1694	0.1888	∼
0.30	5 × 5 × 5	0.32708	0.48215	0.48215	0.63936	0.75009	0.82226	1.0353	1.0658
	6 × 6 × 6	0.33188	0.48322	0.48322	0.64006	0.64742	0.65063	0.88264	0.95325
	7 × 7 × 7	0.33202	0.48327	0.48327	0.64898	0.65075	0.65579	0.89668	0.96697
	8 × 8 × 8	0.33201	0.48327	0.48327	0.65036	0.65043	0.65644	0.89788	0.96654
	9 × 9 × 9	0.33200	0.48327	0.48327	0.64984	0.65043	0.65615	0.89750	0.96657
	10 × 10 × 10	0.33200	0.48327	0.48327	0.64972	0.65043	0.65611	0.89741	0.96654
	11 × 11 × 11	0.33200	0.48327	0.48327	0.64974	0.65043	0.65612	0.89742	0.96654
0.50	5 × 5 × 5	0.69030	0.80359	0.80359	1.0640	1.3612	1.4768	1.5065	1.7208
	6 × 6 × 6	0.70395	0.80536	0.80536	1.0827	1.2275	1.2872	1.4932	1.5888
	7 × 7 × 7	0.70321	0.80546	0.80546	1.0829	1.2403	1.3038	1.4927	1.6116
	8 × 8 × 8	0.70342	0.80546	0.80546	1.0823	1.2428	1.3054	1.4923	1.6109
	9 × 9 × 9	0.70338	0.80545	0.80545	1.0823	1.2423	1.3044	1.4923	1.6109
	10 × 10 × 10	0.70338	0.80545	0.80545	1.0824	1.2424	1.3043	1.4923	1.6109
	11 × 11 × 11	0.70338	0.80545	0.80545	1.0824	1.2423	1.3043	1.4923	1.6109

[1]Srinivas and Rao (1970).

Table 7
Convergence of frequency parameters, $\lambda = \omega\sqrt{\rho c^2/C_{11}}$ of CCCC square orthotropic plates

		Mode sequence number							
c/b	Grid size X × Y × Z	1	2	3	4	5	6	7	8
0.10	5 × 5 × 5	0.07824	0.24117	0.27159	0.30238	0.34121	0.34575	0.37947	0.38529
	6 × 6 × 6	0.07913	0.14302	0.15453	0.20437	0.27216	0.34073	0.35755	0.39650
	7 × 7 × 7	0.07888	0.14461	0.15580	0.20825	0.24043	0.25178	0.27215	0.29022
	8 × 8 × 8	0.07883	0.14101	0.15420	0.20599	0.24445	0.25643	0.27215	0.29539
	9 × 9 × 9	0.07884	0.14105	0.15424	0.20600	0.23173	0.25087	0.27213	0.28608
	10 × 10 × 10	0.07882	0.14103	0.15420	0.20598	0.23213	0.25112	0.27213	0.28646
	11 × 11 × 11	0.07882	0.14101	0.15420	0.20595	0.23181	0.25091	0.27213	0.28626
0.30	5 × 5 × 5	0.43659	0.81503	0.82224	0.96484	1.02370	1.0928	1.1559	1.2082
	6 × 6 × 6	0.44353	0.70711	0.75214	0.81674	0.95787	1.0223	1.0724	1.3009
	7 × 7 × 7	0.44231	0.71215	0.75233	0.81688	0.96623	1.0195	1.0223	1.0768
	8 × 8 × 8	0.44267	0.71333	0.75024	0.81682	0.96598	1.0223	1.0522	1.0766
	9 × 9 × 9	0.44253	0.71310	0.75011	0.81680	0.96574	1.0223	1.0460	1.0766
	10 × 10 × 10	0.44256	0.71321	0.75003	0.81677	0.96577	1.0223	1.0470	1.0766
	11 × 11 × 11	0.44253	0.71315	0.74996	0.81676	0.96568	1.0223	1.0466	1.0766
0.50	5 × 5 × 5	0.83052	1.3594	1.4382	1.6098	1.7061	1.8610	1.9267	2.0640
	6 × 6 × 6	0.85345	1.2863	1.3612	1.3880	1.7041	1.7373	1.7864	2.1239
	7 × 7 × 7	0.85086	1.2960	1.3616	1.3919	1.7040	1.7549	1.7938	1.7997
	8 × 8 × 8	0.85291	1.3022	1.3615	1.3936	1.7040	1.7604	1.7935	1.8681
	9 × 9 × 9	0.85251	1.3016	1.3615	1.3930	1.7040	1.7597	1.7936	1.8593
	10 × 10 × 10	0.85284	1.3026	1.3615	1.3934	1.7040	1.7606	1.7935	1.8626
	11 × 11 × 11	0.85276	1.3025	1.3615	1.3933	1.7040	1.7604	1.7935	1.8619

Table 8
Convergence of frequency parameters, $\lambda = \omega\sqrt{\rho c^2/C_{11}}$ of SCCC square orthotropic plates

		Mode sequence number							
c/b	Grid size X × Y × Z	1	2	3	4	5	6	7	8
0.10	5 × 5 × 5	0.06875	0.21860	0.22046	0.25969	0.30018	0.35062	0.36602	0.38128
	6 × 6 × 6	0.06973	0.13895	0.13898	0.19486	0.22002	0.25924	0.35065	0.37011
	7 × 7 × 7	0.06958	0.14017	0.14055	0.19889	0.22015	0.23485	0.23872	0.25933
	8 × 8 × 8	0.06960	0.13698	0.13992	0.19715	0.22011	0.23909	0.24293	0.25934
	9 × 9 × 9	0.06956	0.13699	0.14000	0.19722	0.22012	0.22991	0.23692	0.25931
	10 × 10 × 10	0.06957	0.13700	0.13986	0.19712	0.22011	0.23034	0.23691	0.25931
	11 × 11 × 11	0.06955	0.13696	0.13991	0.19715	0.22011	0.23001	0.23656	0.25931
0.30	5 × 5 × 5	0.41527	0.66140	0.77937	0.79877	0.96021	1.1020	1.1438	1.1949
	6 × 6 × 6	0.42156	0.66012	0.69153	0.74728	0.77796	0.95138	1.0519	1.1102
	7 × 7 × 7	0.42043	0.66051	0.69799	0.74779	0.77824	0.96004	1.0080	1.0565
	8 × 8 × 8	0.42074	0.66040	0.69874	0.74572	0.77822	0.95940	1.0405	1.0559
	9 × 9 × 9	0.42056	0.66044	0.69856	0.74557	0.77818	0.95924	1.0354	1.0562
	10 × 10 × 10	0.42060	0.66042	0.69851	0.74549	0.77817	0.95915	1.0358	1.0562
	11 × 11 × 11	0.42055	0.66043	0.69853	0.74541	0.77816	0.95912	1.0354	1.0562
0.50	5 × 5 × 5	0.80817	1.1024	1.3001	1.4149	1.6091	1.6758	1.8646	1.9065
	6 × 6 × 6	0.82873	1.1003	1.2781	1.2967	1.3861	1.6757	1.7342	1.7528
	7 × 7 × 7	0.82615	1.1010	1.2882	1.2972	1.3901	1.6726	1.7510	1.7606
	8 × 8 × 8	0.82764	1.1008	1.2925	1.2972	1.3914	1.6756	1.7554	1.7596
	9 × 9 × 9	0.82724	1.1008	1.2920	1.2972	1.3909	1.6755	1.7547	1.7601
	10 × 10 × 10	0.82749	1.1008	1.2925	1.2971	1.3912	1.6753	1.7552	1.7600
	11 × 11 × 11	0.82740	1.1008	1.2925	1.2971	1.3910	1.6753	1.7551	1.7600

Table 9
Convergence of frequency parameters, $\lambda = \omega\sqrt{\rho c^2/C_{11}}$ of CSSS square orthotropic plates

		Mode sequence number							
c/b	Grid size X × Y × Z	1	2	3	4	5	6	7	8
0.10	5 × 5 × 5	0.05562	0.16072	0.19200	0.21494	0.22475	0.28137	0.31041	0.34832
	6 × 6 × 6	0.05646	0.10575	0.13283	0.16107	0.17506	0.19372	0.28117	0.31775
	7 × 7 × 7	0.05652	0.10697	0.13399	0.16109	0.17853	0.18673	0.19372	0.23140
	8 × 8 × 8	0.05660	0.10771	0.13377	0.16109	0.17873	0.19154	0.19368	0.23578
	9 × 9 × 9	0.05654	0.10761	0.13386	0.16109	0.17879	0.19136	0.19368	0.23341
	10 × 10 × 10	0.05658	0.10757	0.13372	0.16109	0.17864	0.19106	0.19368	0.23341
	11 × 11 × 11	0.05655	0.10756	0.13378	0.16109	0.17869	0.19063	0.19368	0.23307
0.30	5 × 5 × 5	0.34448	0.48215	0.57585	0.77497	0.82396	0.84339	1.04790	1.06580
	6 × 6 × 6	0.35147	0.48322	0.58101	0.64281	0.66310	0.84280	0.88681	0.95325
	7 × 7 × 7	0.35104	0.48327	0.58102	0.65138	0.67083	0.84195	0.90119	0.96697
	8 × 8 × 8	0.35139	0.48327	0.58091	0.65296	0.67158	0.84196	0.90271	0.96654
	9 × 9 × 9	0.35125	0.48327	0.58091	0.65236	0.67145	0.84199	0.90234	0.96657
	10 × 10 × 10	0.35133	0.48327	0.58091	0.65228	0.67141	0.84199	0.90227	0.96654
	11 × 11 × 11	0.35129	0.48327	0.58091	0.65229	0.67145	0.84199	0.90230	0.96654
0.50	5 × 5 × 5	0.69847	0.80359	0.95928	1.3838	1.4023	1.5082	1.6251	1.7433
	6 × 6 × 6	0.71560	0.80536	0.96789	1.2359	1.2891	1.4013	1.5888	1.6355
	7 × 7 × 7	0.71442	0.80546	0.96794	1.2489	1.3057	1.4000	1.6116	1.6353
	8 × 8 × 8	0.71549	0.80546	0.96774	1.2529	1.3078	1.4000	1.6109	1.6363
	9 × 9 × 9	0.71527	0.80545	0.96775	1.2525	1.3067	1.4000	1.6109	1.6363
	10 × 10 × 10	0.71546	0.80545	0.96775	1.2529	1.3067	1.4000	1.6109	1.6362
	11 × 11 × 11	0.71542	0.80545	0.96775	1.2529	1.3067	1.4000	1.6109	1.6362

References

Bert, C.W., Malik, M., 1996. Differential quadrature method in computational mechanics: a review. Appl. Mech. Rev. 49 (1), 1–28.

Bert, C.W., Jang, S.K., Striz, A.G., 1988a. Two new approximate methods for analyzing free vibration of structural components. AIAA J. 26, 612–618.

Bert, C.W., Striz, A.G., Jang, S.K., 1998b. Nonlinear deflection of rectangular plates by differential quadrature. Int. Conf. Computational Eng. Sci., vol. 1, Chap. 23, iii.1–iii.4, Atlanta.

Bert, C.W., Jang, S.K., Striz, A.G., 1989. Nonlinear bending analysis of orthotropic rectangular plates by the method of differential quadrature. Comput. Mech. 5, 217–226.

Bisplinghoff, R.L., Mar, J.W., Pian, T.H.H., 1965. Statics of Deformable Solids. Addison-Wesley.

Chen, W.L., 1994. A new approach in structural analysis: the quadrature element method. Ph.D. dissertation. University of Oklahoma, Oklahoma.

Du, H., Lim, M.K., Lin, R.M., 1994. Application of generalized differential quadrature method to structural problems. Int. J. Numer. Methods Eng. 37, 1881–1896.

Du, H., Liew, K.M., Lim, M.K., 1996. Generalized differential quadrature method for buckling analysis. ASCE J. Eng. Mech. 122, 95–100.

Farsa, J., 1991. Development of differential quadrature technique for the fundamental frequency analysis of tapered orthotropic, anisotropic and laminated plates. Ph.D. dissertation. University of Oklahoma, Oklahoma.

Han, J.-B., Liew, K.M., 1995. Static Response of Mindlin plates on Plasternak foundations: the generalised differential quadrature solution. Proceedings of International Conference on Mechanics of Solids and Materials in Engineering B, 580–585, 16–18 June, Singapore.

Iyengar, K.T.S.R., Chandrashekhara, K., Sebastian, V.K., 1974. On the analysis of thick rectangular plates. Ingenieur Archiv. 43, 317–339.

Jang, S.K., 1987. Application of differential quadrature to the analysis of structural components. Ph.D. dissertation. University of Oklahoma, Oklahoma.

Jang, S.K., Bert, C.W., Striz, A.G., 1989. Application of differential quadrature to static analysis of structural components. Int. J. Numer. Methods Eng. 28, 561–577.

Leissa, A.W., Zhang, Z.D., 1983. On the three-dimensional vibrations of the cantilevered rectangular parallelepiped. J. Acous. Soc. of America 73, 2013–2021.

Liew, K.M., Hung, K.C., Lim, M.K., 1993. A continuum three-dimensional vibration analysis of thick rectangular plates. Int. J. Solids Struct. 30, 3357–3379.

Liew, K.M., Hung, K.C., Lim, M.K., 1994. Three-dimensional vibration of rectangular plates: variance of simple support conditions and influence of in-plane inertia. Int. J. Solids Struct. 31, 3233–3247.

Liew, K.M., Hung, K.C., Lim, M.K., 1995a. Three-dimensional vibration of rectangular plates: effects of thickness and edge constraints. J. Sound Vibr. 182, 5, 709–727.

Liew, K.M., Hung, K.C., Lim, M.K., 1995b. Free vibration studies on stress-free three-dimensional elastic solids. ASME J. Appl. Mech. 62, 159–165.

Malik, M., 1994. Differential quadrature method in computational mechanics: new developments and applications. Ph.D. dissertation. University of Oklahoma, Oklahoma.

Malik, M., Bert, C.W., 1995. Differential quadrature analysis of free vibration of symmetric cross-ply laminates with shear deformation and rotary inertia. Shock Vibr. 2, 321–338.

Malik, M., Bert, C.W., 1998. Three-dimensional elasticity solutions for free vibrations of rectangular plates by the differential quadrature method. Int. J. Solids Struct. 35, 299–318.

Quan, J.R., Chang, C.T., 1989a. New insights in solving distributed system equations by the quadrature methods—I. Analysis. Comput. Chem. Eng. 13, 779–788.

Quan, J.R., Chang, C.T., 1989b. New insights in solving distributed system equations by the quadrature methods—II. Numerical experiments. Comput. Chem. Eng. 13, 779–788.

Shu, C., Richards, B.E., 1992. Application of generalized differential quadrature to solve two-dimensional incompressible Navier–Stokes equations. Int. J. Numer. Methods Fluids 15, 791–798.

Srinivas, S., Rao, A.K., 1969. Buckling of thick rectangular plates. AIAA Journal 7, 1645–1646.

Srinivas, S., Rao, A.K., 1970. Bending, vibration and buckling of simply supported thick orthotropic rectangular plates and laminates. Int. J. Solids Struct. 6, 1463–1481.

Srinivas, S., Rao, A.K., 1973. Flexure of thick rectangular plates. ASME J. Appl. Mech. 40, 298–299.
Srinivas, S., Rao, A.K., Rao, C.V., 1969. Flexure of simply supported thick homogeneous and laminated rectangular plates. ZAMM 49, 449–458.
Srinivas, S., Rao, C.V., Rao, A.K., 1970. An exact analysis for vibration of simply supported homogeneous and laminated thick rectangular plates. J. Sound Vibr. 12, 187–199.
Striz, A.G., Jang, S.K., Bert, C.W., 1988. Nonlinear bending analysis of thin plates by differential quadrature. Thin-walled Struct. 31, 2807–2818.
Teo, T.M., 1998. Three-dimensional analysis of plate panels based on differential quadrature method. M.Eng. thesis. Nanyang Technological University, Singapore.
Teo, T.M., Liew, K.M., 1997. Free-vibration of plate panels with three-dimensional flexibility. The 11th Technical Exchange and Advisory Meeting on Marine Structures. Singapore, pp. 129–134.
Wang, X., 1995. Differential quadrature for buckling analysis of laminated plates. Comput. Struct. 57, 715–719.
Wang, X., Yang, J., Xiao, J., 1995. On free vibration analysis of skew plates with non-uniform thickness by the differential quadrature method. J. Sound Vibr. 184, 547–551.
Wittrick, W.H., 1987. Analytical, three-dimensional elasticity solutions to some plate problems, and some observations on Mindlin's plate theory. Int. J. Solids Struct. 23, 4, 441–464.
Young, P.G., Dickinson, S.M., 1995. Free vibration of a class of homogeneous isotropic solids. ASME J. Appl. Mech. 62, 706–708.